J Sol-Gel Sci Technol (2017) 84:507–514
DOI 10.1007/s10971-017-4380-5

INVITED PAPER: NANO- AND MACROPOROUS MATERIALS (AEROGELS, XEROGELS, CRYOGELS, ETC.)

Highly thermally stable alumina-based aerogels modified by partially hydrolyzed aluminum tri-sec-butoxide

Wenbing Zou[1] · Xiaodong Wang[1] · Yu Wu[1] · Guoqing Zu[1] · Liping Zou[1] · Rongyan Zhang[2] · Xiandong Yao[2] · Jun Shen[1]

Received: 8 December 2016 / Accepted: 30 March 2017 / Published online: 17 April 2017

Abstract Highly thermally stable alumina-based aerogels are synthesized by the acetone–aniline in situ water formation method and modified by partially hydrolyzed aluminum tri-sec-butoxide at different temperatures (25, 45, and 60 °C). The effects of modification, especially modification temperature, on microstructure and thermal stability of alumina-based aerogels are investigated. After the modification, the morphologies of alumina-based aerogels change from the network structures with interconnected needle-like particles to those with stacked sheet-like particles, resulting in a better heat resistance. The thermal stability of alumina-based aerogels enhances with the increasing modification temperature, whereas the high temperature (more than 60 °C) would lead to the dissolution of wet gels during the modification process due to the high solubility. After annealing at 1200 °C for 2 h, the 45 °C-modified alumina-based aerogel exhibits the best thermal stability with the lowest linear shrinkage of ~7% and the highest specific surface area of 154 m^2/g. In addition, the modified aerogels remain in the θ-Al_2O_3 phase while the unmodified one transforms into α-Al_2O_3 phase after 1300 °C annealing. The alumina-based aerogels are further reinforced by incorporating with mullite fiber felt and TiO_2. The obtained composites show ultralow thermal conductivities of 0.065, 0.086, and 0.118 W/mK at 800, 1000, and 1200 °C, respectively.

Graphical Abstract

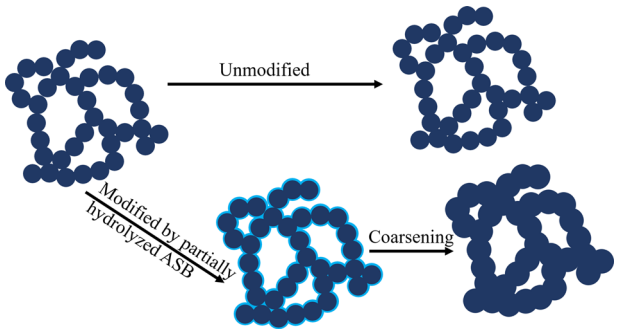

Keywords Alumina-based aerogels · Thermal stability · Modification of partially hydrolyzed ASB · Composite

Abbreviations

ASB	aluminum tri-sec-butoxide
TMEO	trimethylethoxysilane
EtOH	ethanol

1 Introduction

Owing to the large specific surface area, ultralow thermal conductivity, catalytic activity and better heat resistance than silica aerogel, alumina-based aerogels have drawn great interest in the applications of high temperature thermal insulation and catalysts over the past few decades [1–10]. However, metastable alumina phase will easily transform to

✉ Xiaodong Wang
xiaodong_wang@tongji.edu.cn

✉ Jun Shen
shenjun67@tongji.edu.cn

[1] Shanghai Key Laboratory of Special Artificial Microstructure Materials and Technology, School of Physics Science and Engineering, Tongji University, Shanghai 200092, China

[2] Nano Technology Co. Ltd, Zhejiang 312366, China

crystallographic stable α-Al_2O_3 phase with a great loss of surface area and collapse of the porous structure after heating above 1150 °C [11], which limits their high temperature applications. Therefore, many efforts have been dedicated to improving the thermal stability of alumina-based aerogels [12–22].

It has been reported that incorporation of silica is an effective method to improve the thermal stability of alumina aerogel [11–13, 16, 19–22]. For example, Horiuchi et al. [11] used aluminum tri-isopropoxide and tetraethoxysilane as precursors to prepare silica-doped alumina (SDA) aerogels with a surface area of 150 m^2/g after heated at 1200 °C. Silica was found to be effective for inhibiting the crystal growth and phase transition of alumina, thus maintaining large specific surface area after heat treatment. Osaki et al. [16] prepared alumina cryogels with a dopant of 10 wt% silica from aqueous boehmite sol and found that γ-Al_2O_3 phase still remained after heating at 1200 °C for 5 h and the surface area were 47 m^2/g. Mardkhe et al. [21] produced 5 wt% SDA with a high surface area of 160 m^2/g after heated at 1100 °C that silica improved the thermal stability of alumina by formation of an interfacial silica–alumina phase between primary crystallite in the agglomerate. It has also been found that the addition of some rare-earth, such as La and Ba, can inhibit the phase transition and the formation of α-Al_2O_3, thus improving the thermal stability of alumina aerogels [23, 24]. Mizushima et al. [23] added SiO_2, La_2O_3, BaO, and SiC whisker into alumina aerogels to enhance the specific surface area of the alumina aerogel at a temperature over 1200 °C.

Besides, Zu et al. [25, 26] proposed a series of modification techniques to enhance the thermal stability of SDA aerogels to 1300 °C by inhibiting the crystal growth and the phase transition of alumina aerogels. The resulting alumina-based aerogel shrinks little and possesses a high specific surface area of 136 m^2/g after heated at 1200 °C for 2 h. In particular, partially hydrolyzed alkoxide modification plays an important role in the process of modification, thus affecting the properties of the resulting aerogels. However, similar to the aging process, the modification is a dynamic process with the dissolution and re-precipitation [27], which is influenced by temperature, pH, and concentration. Hence, it is necessary to further study the influence of modification temperature on the thermal stability of alumina-based aerogels.

In this work, heat resistant alumina-based aerogels were prepared by modification of partially hydrolyzed aluminum tri-sec-butoxide (ASB) at different temperatures (25, 45, and 60 °C) and ethanol supercritical fluid drying. The effects of modification, especially modification temperature on microstructure, phase transition, and the thermal stability of alumina-based aerogels were investigated. In order to improve the mechanical properties and reduce their high-temperature thermal conductivity, the alumina-based aerogels were reinforced by mullite fiber felt and TiO_2 particles, leading to excellent heat resistance and ultralow high-temperature thermal conductivities.

2 Experimental

2.1 Synthesis

The alumina-based wet gels were prepared via acetone-aniline in situ water formation method [26]. Firstly, ASB was added into the mixture of ethanol and distilled water at 60 °C with stirring and then cooled down to room temperature. Secondly, ethanol-diluted nitric acid was added into the mixture with stirring. Thirdly, an appropriate amount of acetone, aniline, and trimethylethoxysilane (TMEO) was added into the above mixture. The molar ratio of ASB, EtOH, H_2O, HNO_3, acetone, aniline, and TMEO was kept at 1:3.5:0.4:0.02:1.8:1.8:0.2. After stirring for 10 min, the mixture was transferred into glass beakers and then gelation occurred at room temperature (25 °C) within 2 h. After aging and solvent exchanged, the wet gels were soaked in the solution of partially hydrolyzed ASB at different temperatures (25, 45 and 60 °C) for 3 days. The solution of partially hydrolyzed ASB was prepared by dissolving ASB in the mixture of ethanol and distilled water in a molar ratio of ASB, EtOH and H_2O = 1:110:0.5. Correspondingly, the un-modified samples were directly soaked in ethanol at room temperature (25 °C) for the same time. The wet gels modified at 60 °C dissolved, which is not possible to be dried by supercritical drying. The samples of un-modified, modified at room temperature (25 °C) and modified at 45 °C were labeled as A0, A25 and A45, respectively. All these wet gels were dried by supercritical ethanol to obtain the alumina-based aerogels. The as-prepared aerogels were heated to different temperatures (1000, 1200, and 1300 °C) with the same heating rate of 10 °C/min, kept for 2 h then cooled naturally in muffle furnaces. The alumina-based aerogels are further reinforced by incorporating with polycrystalline mullite fiber felt and opacifier (TiO_2). The mullite fiber was purchased from Tianjin Morgan Kundom High-tech Development Co., Ltd. (China). The composites are composed of 48 wt% mullite fiber, 43 wt% Al_2O_3-based aerogels and 9 wt% TiO_2 particles.

2.2 Characterizations

The morphology of the aerogels was characterized by scanning electron microscopy (XL30FEG, Philips, The Netherlands) and a transmission electron microscope (JEOL-1230, Jeol Ltd., Japan). The crystal phase of the

aerogels were analyzed by powder X-ray diffraction (XRD) in a Rigata/max-C diffractometer using Cu-Kα radiation (DX-2700, Hao Yuan Instrument, China). The specific surface area and pore-size distribution were measured by a N_2 adsorption analyzer (TriStar 3000, Quantachrome Instruments, USA) using the BET N_2 adsorption/desorption technique. The compression modulus was measured by a universal tensile testing machine (CMT5000, Mattes, China). The high-temperature thermal conductivity was measured by a flat thermal conductivity instrument (Pbd-02p, China).

3 Results and discussion

3.1 The mechanism of partially hydrolyzed ASB modification

Figure 1 shows the schematic of modification of partially hydrolyzed ASB. The surface of alumina-based gels were covered by active OH groups which makes it possible to be modified by reaction with OH groups [27]. The partially hydrolyzed ASB can be expressed as $Al(OH)_x(OC_4H_9)_{3-x}$. When the wet gels are immersed in the solution of partially hydrolyzed ASB, $Al(OH)x(OC_4H_9)_{3-x}$ will react with the -OH groups on the surface of alumina nanoparticles, involving in dehydration and dealcoholization reactions as follows:

$$-Al-OH+(OH)_xAl(OC_4H_9)_{3-x} \rightarrow -Al-O-Al(OH)_{x-1}(OC_4H_9)_{3-x}+H_2O$$

$$-Al-OH+(OC_4H_9)_{3-x}Al(OH)_x \rightarrow -Al-O-Al(OH)_x(OC_4H_9)_{2-x}+C_4H_9OH$$

As the reaction processed, the size of alumina nanoparticle gets larger and the strength of skeleton is enhanced. Alumina gels are composed of alumina secondary particles connected by necks. As we know, the solubility of the surface of particles is higher than the surface of necks [27]. Therefore, a progress of dissolution and re-precipitation happened during the modification results in the coarsening of necks that strengthen the skeletons of alumina gels. Apart from this, the solubility of wet gels will significantly increase with the increase of the temperature.

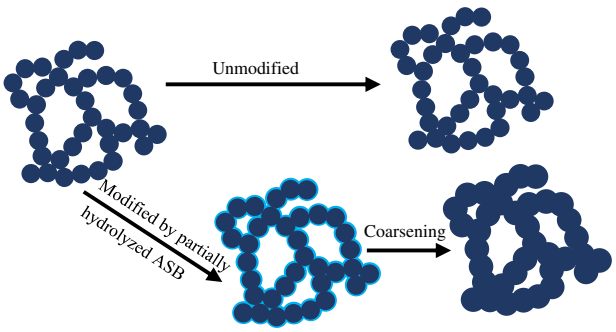

Fig. 1 Schematic of alumina-based wet gels modified with partially hydrolyzed ASB

3.2 The effect of modification temperature on morphology

Figure 2 exhibits the sample images of the obtained alumina-based aerogels before and after heat treatment at 1200 °C for 2 h. The as-prepared aerogels are brown and fade after heated at 1200 °C due to the decomposition of the carbonaceous organic groups in the aerogels [29]. As shown in Table 1 and Fig. 2, after heated at 1200 °C the unmodified aerogel A0 shrinks as high as 38%, whereas the A25 and A45 shrinks only 14 and 7%, respectively. It suggested that the modification with partially hydrolyzed ASB can significantly reduce the shrinkage of alumina-based aerogels during the heat treatment and the effect of modification increased with the elevation of modification temperature.

Figures 3 and 4 show the morphology of the alumina-based aerogels before and after heat treatment at 1200 °C. As seen from the SEM (Fig. 3a–c), the morphology of alumina-based aerogels change from the network structures with interconnected spheroidal agglomerates to those with stacked sheet-like agglomerates after the modification. After heat treatment at 1200 °C for 2 h, the unmodified sample A0 becomes dense with the collapse of pore structures, whereas the modified samples remain a loose structure although the sheet-like agglomerates grow larger. Besides, the stacking structure of A45 is more loosely than A25. In the TEM images, we also clearly observed the morphology change of alumina nanoparticles. The unmodified alumina-based aerogel (A0) exhibits randomly interconnected network, which is made up of needle-like nanoparticles, whereas the modified ones (A25 and A45) show larger sheet-like particles. As mentioned in 3.1, after the modification of partially hydrolyzed ASB, the alumina nanoparticles grow larger and the necks become coarser. It is worth noting that A45 has larger and thicker sheet-like nanoparticles. After heat treatment at 1200 °C for 2 h, the unmodified alumina-based aerogel is composed of spheroidal and rod-like particles, whereas the modified ones are composed of larger sheet-like particles and some rod-like particles. The morphology evolution illustrated that the modification brings the alumina-based aerogels lager sheet-like particles and stronger skeletons, which avoid their sintering at high temperature.

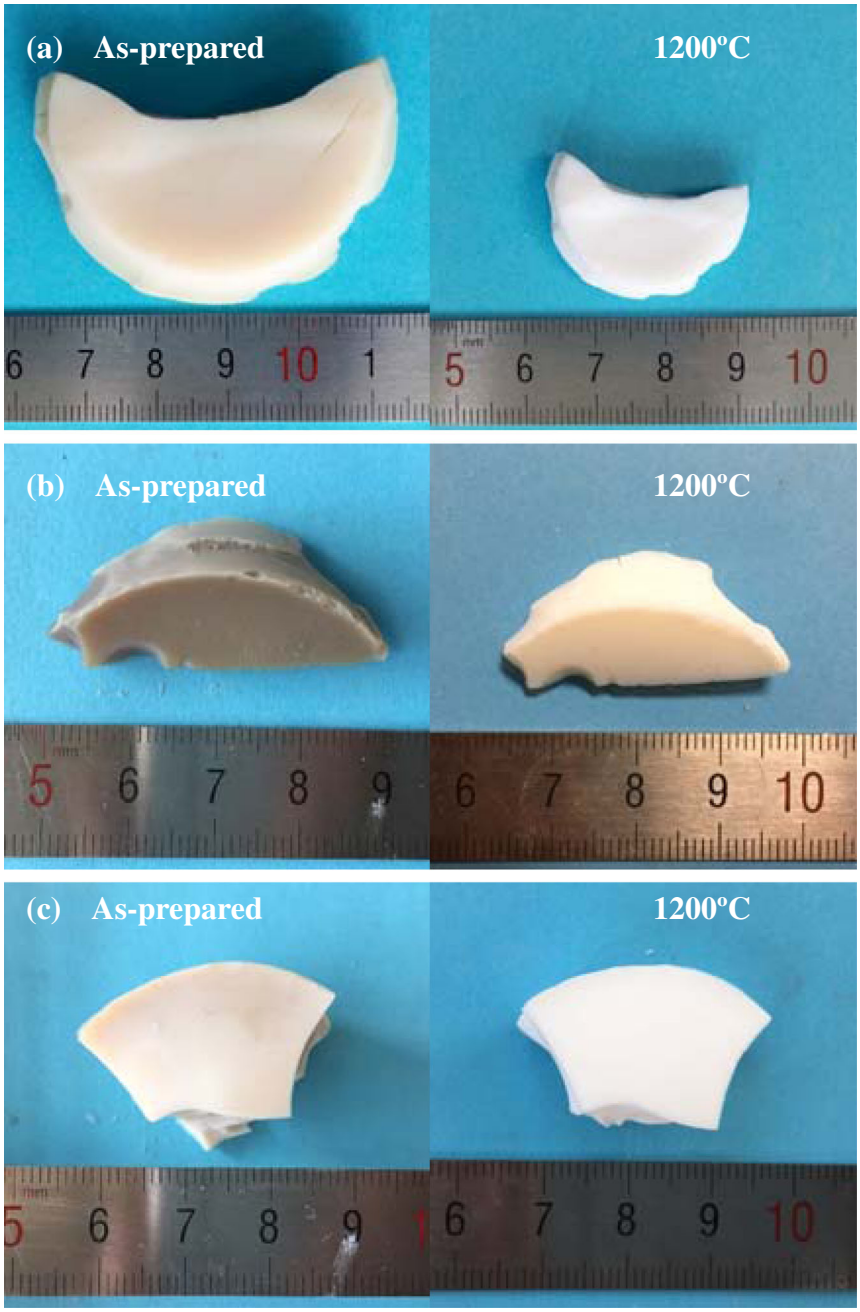

Fig. 2 Sample images of the alumina-based aerogels before and after heat treatment at 1200 °C for 2 h, respectively. **a** A0; **b** A25; **c** A45

3.3 The effect of modification temperature on specific surface area and pore structure

As shown in Table 1, the density of dried alumina-based aerogels increases a little and the specific surface area decreases from 304 to 200 m^2/g after the modification. The reason is that the modification leads to the formation of lager sheet-like particles, which reduces the mesopores and the specific surface area. After heat treatment at 1200 °C, the specific surface area of unmodified aerogel A0 dramatically decreases from 304 to 72 m^2/g, whereas those of the modified aerogels A25 and A45 remain 139 and 154 m^2/g, respectively. Moreover, the 45 °C-modified aerogel A45 possesses a lager specific surface area than the 25 °C-modified sample A25 after heat treatment at 1200 °C. This indicates that modification effectively enhances the specific surface area of alumina-based aerogels at higher temperature and an appropriate temperature is important for the modification.

Figure 5 presents the N_2 adsorption/desorption isotherms and pore size distribution of alumina-based aerogels before and after heat treatment. The isotherms are type IV curves

Table 1 Textural properties of the alumina-based aerogels after supercritical drying (300 °C) and heat treatment at 1200 °C

Sample	Modificat-ion	Density[a] (mg/cm^3)	S_{BET}[b] (m^2/g)		d[c] (nm)		$\Delta L/L_0$[d] (%)	
			300 °C	1200 °C	300 °C	1200 °C	1000 °C	1200 °C
A0	No	102	304	72	28.0	14.2	9	38
A25	25 °C	124	232	139	16.9	12.2	2	14
A45	45 °C	139	200	154	15.2	–	0	7

[a] The bulk density of dried aerogels, which was determined by $\rho = m/V$

[b] BET-specific surface area

[c] Average pore diameter obtained from nitrogen desorption branch and Barrett–Joyner–Halenda (BJH) method

[d] Shrinkage after heat treatment. L_0 is the original diameter of the sample and ΔL is the diameter decrement

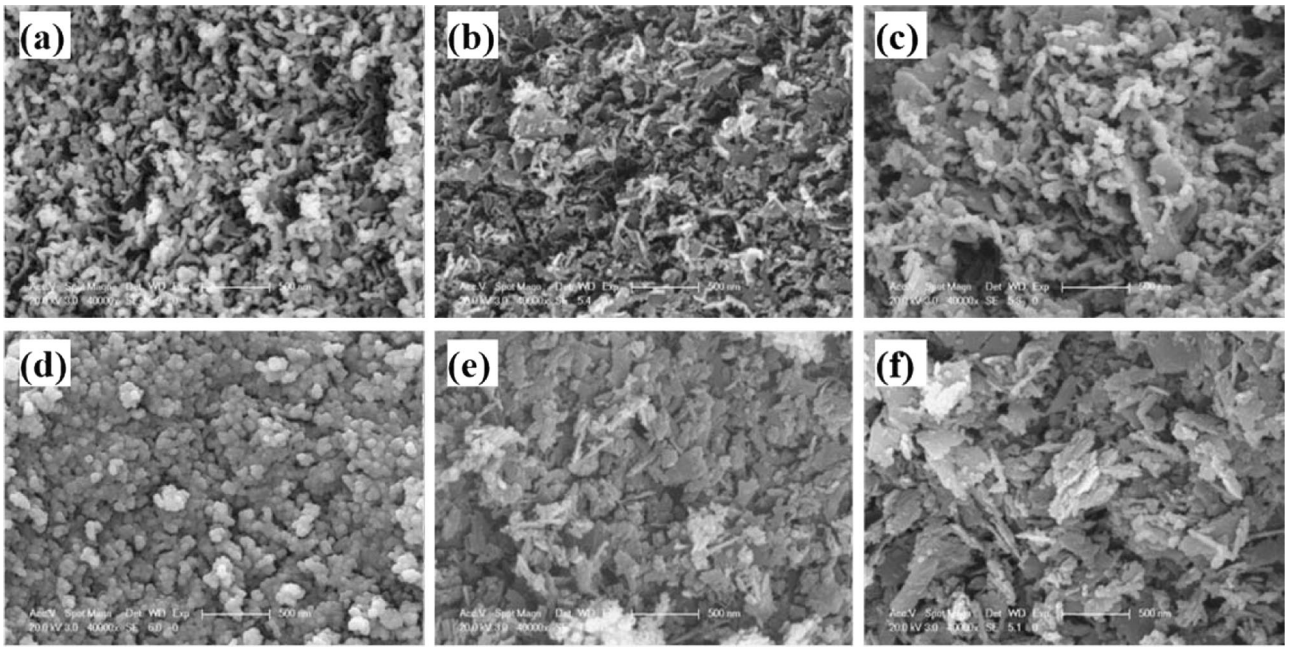

Fig. 3 SEM images of the alumina-based aerogels before and after heat treatment at 1200 °C for 2 h. **a** A0;.**b** A25. **c** A45. **d** A0–1200 °C. **e** A25–1200 °C. **f** A45–1200 °C

with type H3 hysteresis loop in the IUPAC classification, which is the characteristic of a mesoporous structure with aggregates of slit-shaped pores induced by plate-like particles [30]. As displayed in Table 1 and Fig. 4d–f, the average pore diameters of the modified alumina-based aerogels are smaller than that of the unmodified samples. The modified aerogel A25 exhibits smaller variation of pore size distribution than the unmodified aerogel A0 before and after heat treatment at 1200 °C, which confirms that the pore structure of modified alumina-based aerogels can be well reserved after heated at elevated temperature. However, the pore size distribution of A45 shows no maximum in the testing range, and becomes wider after heat treatment at 1200 °C, which probably attribute to the collapse of mesopores and the formation of large pores above 100 nm.

3.4 The effect of partially hydrolyzed ASB modification on crystal phase

Figure 6 presents the XRD patterns of the alumina-based aerogels after heating at different temperatures. All the as-prepared aerogels are composed of boehmite AlO(OH) (PDF no. 21-1307) [31], which designated as b in Fig. 6. A45 shows more narrow and intense peaks, indicating higher degree of crystallinity than that of A25 and unmodified sample A0. It is well known that the as-prepared metastable boehmite undergoes a series of phase transitions to stable α-Al_2O_3 with the increasing annealing temperature (boehmite $\rightarrow \gamma \rightarrow \theta \rightarrow \alpha$-$Al_2O_3$) [31]. After heating at 1000 °C for 2 h, all the alumina-based aerogels change to the mixed

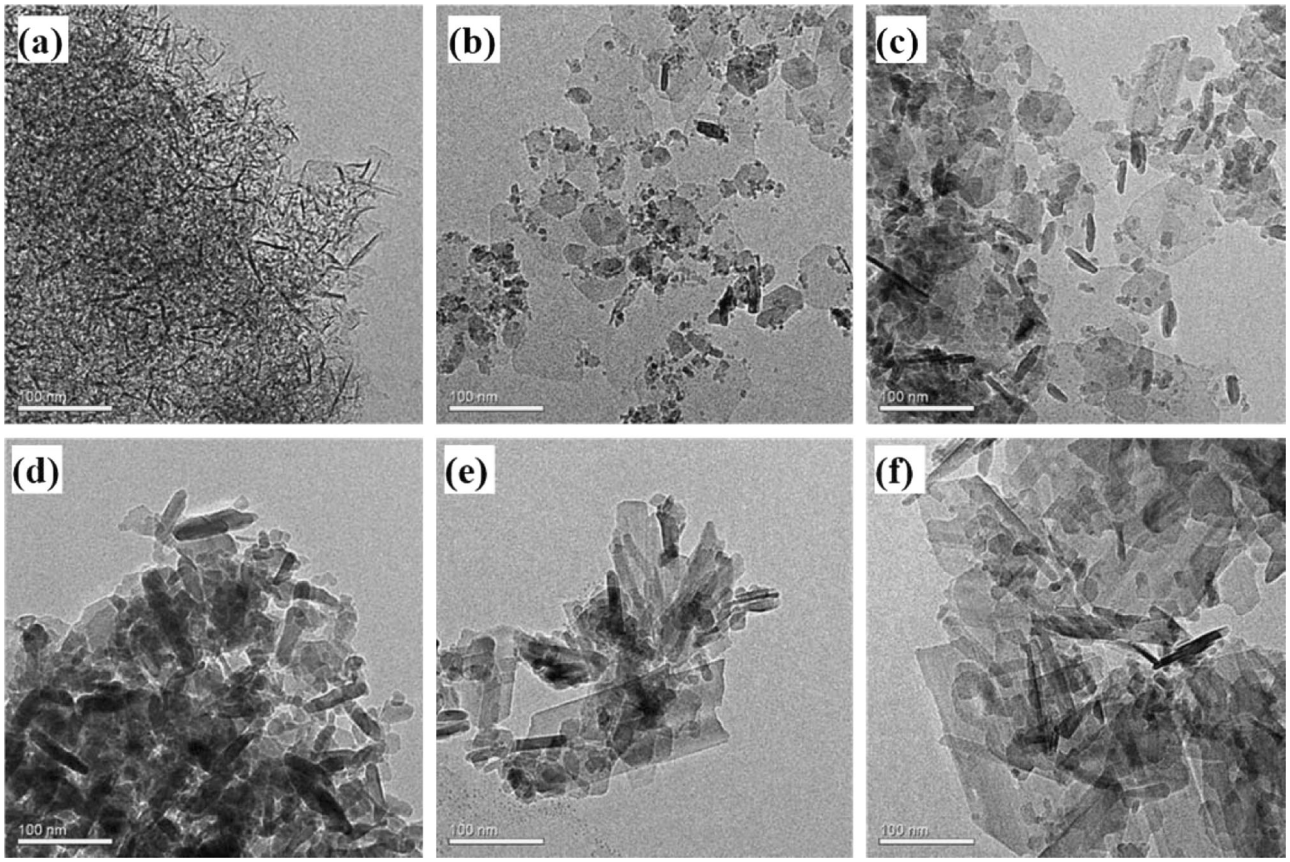

Fig. 4 TEM images of the alumina-based aerogels before and after heat treatment at 1200 °C for 2 h. **a** A0. **b** A25. **c** A45. **d** A0–1200 °C. **e** A25–1200 °C. **f** A45–1200 °C

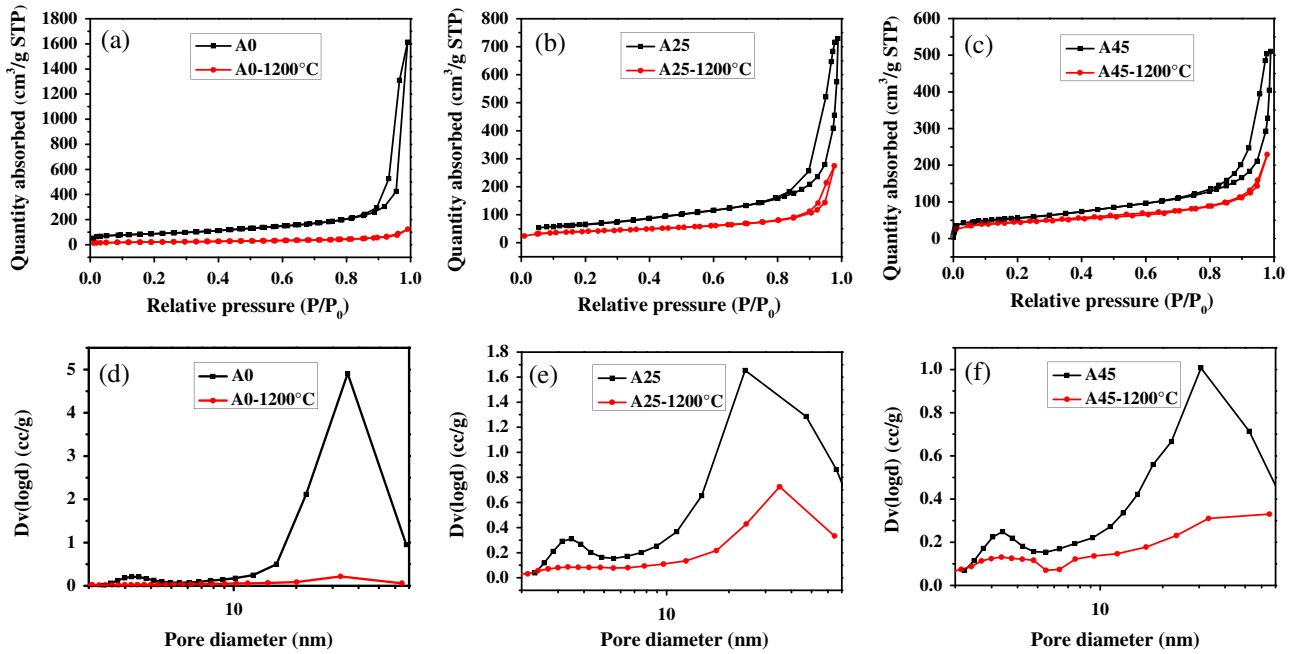

Fig. 5 N_2 adsorption/desorption isotherms of aerogels **a** A0, **b** A25, and **c** A45 before and after heated at 1200 °C for 2 h. BJH pore size distribution of aerogels **d** A0, **e** A25, and **f** A45 before and after heated at 1200 °C for 2 h

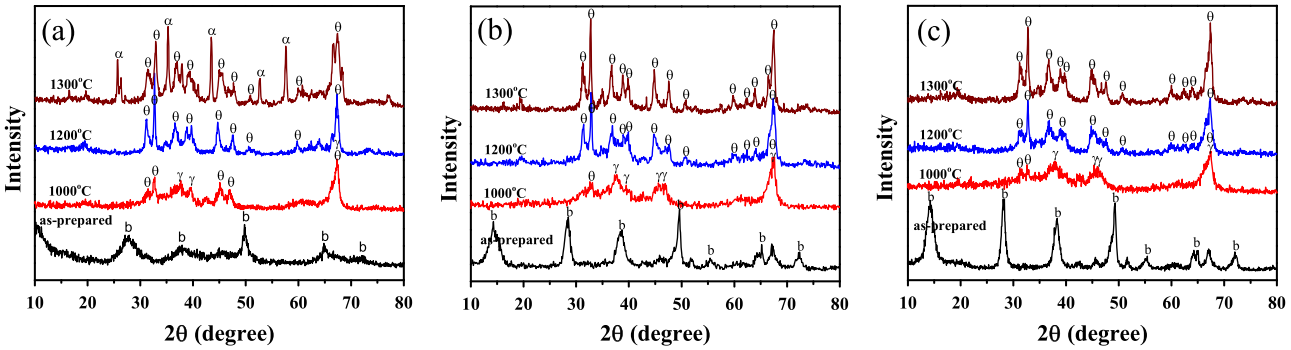

Fig. 6 The XRD patterns of the alumina-based aerogels before and after heated at 1000, 1200, and 1300 °C for 2 h, respectively. **a** A0. **b** A25. **c** A45

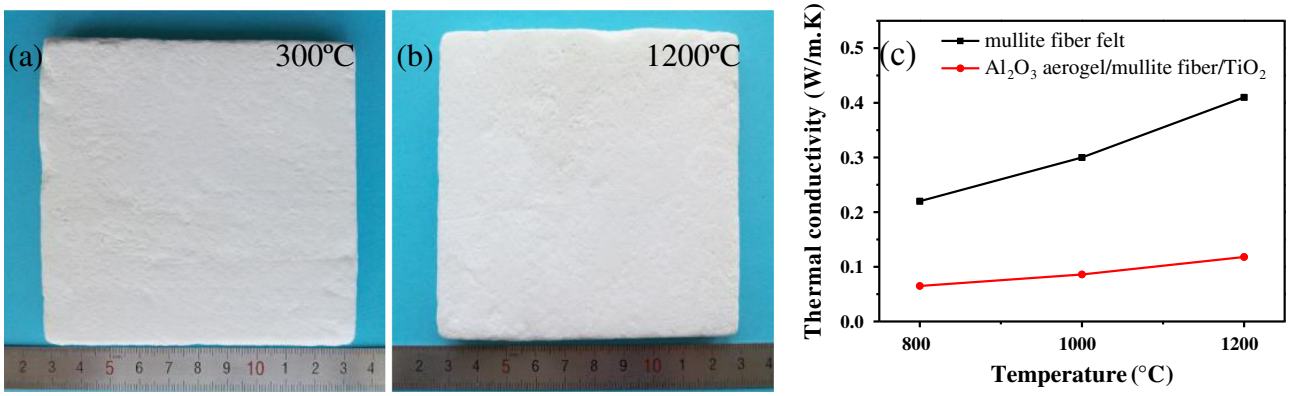

Fig. 7 Photographs of the alumina-based aerogels reinforced by mullite fiber felt and TiO_2 (10 cm × 10 cm × 2 cm) before (**a**) and after (**b**) heated at 1200 °C, and **c** high temperature thermal conductivities for the commercial polycrystalline mullite fiber and alumina aerogel/mullite fiber/TiO_2 composites

phase of γ-Al_2O_3 (PDF no. 47-1308) and θ-Al_2O_3 (PDF no. 35-0121). After heating at 1200 °C for 2 h, all the samples transform to θ-Al_2O_3 phase. After further heating at 1300 °C for 2 h, A25 and A45 still remain in θ-Al_2O_3 phase, while A0 transforms into α-Al_2O_3 phase (PDF no. 46-1212), which indicates that the phase transition of θ-Al_2O_3 to α-Al_2O_3 at 1300 °C is inhibited by modification. The reason could be explained as follows. The vacancy concentration on the neck of alumina-based aerogels is large, which is favorable for rearrangement of atoms and nucleation of α-Al_2O_3 [11]. The necks among the alumina nanoparticles are coarsened by modification of partially hydrolyzed ASB, reducing the nucleation sites of α-Al_2O_3, thereby inhibiting the formation of the α-Al_2O_3 phase [26].

3.5 Alumina-based aerogel reinforced by mullite fiber felt and TiO_2 particles

Alumina-based aerogels are very brittle, which limits their practical application. In order to improve the mechanical properties of alumina aerogels, they are reinforced by mullite fibers felts (with diameter of ~3 μm). Moreover, we use TiO_2 particles (with diameter of ~0.4 μm) as opacifier to block the thermal radiation at elevated temperature. Figure 7a, b shows the sample photos of the alumina-based aerogels reinforced by mullite fiber felt and TiO_2 particles before and after heated at 1200 °C for 2 h. There is no linear shrinkage, indicating that the obtained composite materials have excellent thermal stability. The compression modulus of the composite material is 1.46 MPa which is much higher than the mullite fiber of 0.05 MPa. As presented in Fig. 7c, the high temperature thermal conductivities of alumina aerogels reinforced by mullite fiber and TiO_2 at 800, 1000, and 1200 °C are 0.065, 0.086, and 0.118 W/m·K, respectively, which are much lower than those of the commercial polycrystalline mullite fiber [25] (0.22, 0.30, and 0.41 W/m·K, respectively). The commercial polycrystalline mullite fiber does not contain TiO_2 opacifier. The high temperature thermal conductivities of obtained composite materials are lower than the core−shell Al_2O_3 aerogel/mullite fiber composite, as reported by Zu et al. [25]. With such excellent thermal insulation properties, the composite materials are expected to be applied for high temperature thermal insulations.

4 Conclusions

In summary, the effects of partially hydrolyzed ASB modification, especially modification temperature, on microstructure and thermal stability of alumina-based aerogels are comprehensively investigated. After the modification, the morphologies of alumina-based aerogels change from the network structures with needle-like particles to those with larger stacked sheet-like particles, resulting in a better heat resistance. In addition, the modification with partially hydrolyzed ASB inhibits the phase transition of metastable alumina-based aerogels to stable α-Al_2O_3, thus reduces the loss of their specific surface area at elevated temperature. The process of the modification is greatly influenced by the modification temperature. When the temperature is above 60 °C, the wet gel dissolves which makes it difficult to obtain aerogels by supercritical drying. The 45 °C modified aerogel shows the best thermal stability with the lowest linear shrinkage of ~ 7% and the highest specific surface area of 154 m^2/g after heated at 1200 °C for 2 h. The obtained alumina-based aerogels reinforced by mullite fiber felt and TiO_2 particles have no shrinkage after heated at 1200 °C for 2 h, and exhibit ultra-low high temperature thermal conductivities of 0.065, 0.086, and 0.118 W/mK at 800, 1000, and 1200 °C, respectively. The resulting aerogels and their composites are promising candidates for high temperature thermal insulators.

Acknowledgements This work was supported by the Major Science and Technology Projects of Zhejiang Province (2014C01030), "Chen Guang" project supported by Shanghai Municipal Education Commission and Shanghai Education Development Foundation (Grant No. 14CG19) and National Key Technology Research and Development Program of China (2013BAJ01B01).

Compliance with ethical standards

Conflict of Interest The authors declare that they have no competing interests.

References

1. Yoldas BE (1975) Am Ceram Soc Bull 54(3):289–290
2. Yoldas BE (1975) Am Ceram Soc Bull 54(3):286–288
3. Hirashima H, Kojima C, Imai H (1997) J Solgel Sci Technol 8(1-3):843–846
4. Kim J-H, Suh DJ, Park T-J, Kim K-L (2000) Appl Catal A Gen 197(2):191–200
5. Suh DJ, Park T-J, Lee S-H, Kim K-L (2001) J Non Cryst Solids 285(1):309–316
6. Pierre AC, Pajonk GM (2002) Chem Rev 102(11):4243–4266
7. Al-Yassir N, Le Van Mao R (2007) Appl Catal A Gen 317 (2):275–283
8. Aegerter MA, Leventis N, Koebel MM (2011) Aerogels handbook. Springer, New York
9. Bang Y, Han SJ, Yoo J, Park S, Choi JH, Lee YJ, Song JH, Song IK (2014) Int J Hydrogen Energy 39(10):4909–4916
10. Wang W, Zhang Z, Zu G, Shen J, Zou L, Lian Y, Liu B, Zhang F (2014) RSC Adv 4(97):54864–54871
11. Horiuchi T, Osaki T, Sugiyama T, Suzuki K, Mori T (2001) J Non Cryst Solids 291(3):187–198
12. Horiuchi T, Chen L, Osaki T, Sugiyama T, Suzuki K, Mori T (1999) Catal Lett 58(2-3):89–92
13. Miller JB, Ko EI (1998) Catal Today 43(1):51–67
14. Poco JF, Satcher JH, Hrubesh LW (2001) J Non Cryst Solids 285 (1):57–63
15. Baumann TF, Gash AE, Chinn SC, Sawvel AM, Maxwell RS, Satcher JH (2005) Chem Mater 17(2):395–401
16. Osaki T, Nagashima K, Watari K, Tajiri K (2007) J Non Cryst Solids 353(24):2436–2442
17. Osaki T, Mori T (2009) J Non Cryst Solids 355(31):1590–1596
18. Osaki T, Yamada K, Watari K, Tajiri K, Shima S, Miki T, Tai Y (2012) J Solgel Sci Technol 61(1):268–274
19. Aravind PR, Mukundan P, Pillai PK, Warrier K (2006) Microporous Mesoporous Mater 96(1):14–20
20. Padmaja P, Warrier K, Padmanabhan M, Wunderlich W, Berry FJ, Mortimer M, Creamer NJ (2006) Mater Chem Phys 95(1):56–61
21. Mardkhe MK, Huang B, Bartholomew CH, Alam TM, Woodfield BF (2016) J Porous Mater 23(2):475–487
22. Wu X, Shao G, Cui S, Wang L, Shen X (2016) Ceram Int 42 (1):874–882
23. Mizushima Y, Hori M (1993) J Mater Res 8(11):2993–2999
24. Yang J, Wang Q, Wang T, Liang Y (2016) RSC Adv 6 (31):26271–26279
25. Zu G, Shen J, Wang W, Zou L, Lian Y, Zhang Z, Liu B, Zhang F (2014) Chem Mater 26(19):5761–5772
26. Zu G, Shen J, Zou L, Wang W, Lian Y, Zhang Z, Du A (2013) Chem Mater 25(23):4757–4764
27. Brinker CJ, Scherer GW (2013) Sol-gel science: the physics and chemistry of sol-gel processing. Academic, New York, NY
28. Leventis N (2007) Acc Chem Res 40(9):874–884
29. Zu G, Shen J, Wei X, Ni X, Zhang Z, Wang J, Liu G (2011) J Non Cryst Solids 357(15):2903–2906
30. Sing KS (1985) Pure Appl Chem 57(4):603–619
31. Boumaza A, Favaro L, Lédion J, Sattonnay G, Brubach J, Berthet P, Huntz A, Roy P, Tétot R (2009) J Solid State Chem 182 (5):1171–1176